



# Respiratory analysis of coupled mitochondria in cryopreserved liver biopsies

Mercedes García-Roche<sup>a,b</sup>, Alberto Casal<sup>b</sup>, Mariana Carriquiry<sup>b</sup>, Rafael Radi<sup>a</sup>, Celia Quijano<sup>a,\*</sup>, Adriana Cassina<sup>a,\*</sup>

<sup>a</sup> Center for Free Radical and Biomedical Research (CEINBIO) and Departamento de Bioquímica, Facultad de Medicina, Universidad de la República, Uruguay

<sup>b</sup> Departamento de Producción Animal y Pasturas, Facultad de Agronomía, Universidad de la República, Uruguay

## ARTICLE INFO

### Keywords:

Cryopreservation  
Mitochondria  
Biopsy  
Oxygen consumption rate  
High-resolution respirometry  
Mitochondrial function

## ABSTRACT

The aim of this work was to develop a cryopreservation method of small liver biopsies for in situ mitochondrial function assessment. Herein we describe a detailed protocol for tissue collection, cryopreservation, high-resolution respirometry using complex I and II substrates, calculation and interpretation of respiratory parameters. Liver biopsies from cow and rat were sequentially frozen in a medium containing dimethylsulfoxide as cryoprotectant and stored for up to 3 months at  $-80^{\circ}\text{C}$ . Oxygen consumption rate studies of fresh and cryopreserved samples revealed that most respiratory parameters remained unchanged. Additionally, outer mitochondrial membrane integrity was assessed adding cytochrome *c*, proving that our cryopreservation method does not harm mitochondrial structure. In sum, we present a reliable way to cryopreserve small liver biopsies without affecting mitochondrial function. Our protocol will enable the transport and storage of samples, extending and facilitating mitochondrial function analysis of liver biopsies.

## 1. Introduction

Mitochondria are eukaryotic cell organelles involved in synthesis and catabolism of metabolites, generation of reactive oxygen species [1,2], regulation of intracellular calcium concentrations [3] and apoptosis [4]. Most importantly they have a predominant role in cell bioenergetics, since these organelles are responsible for most of the ATP generated in many tissues [5].

Mitochondrial electron transport and ATP production by oxidative phosphorylation can be assessed measuring oxygen consumption. Its correct assessment has become a staple concern of mitochondrial physiology research on neurodegenerative diseases [6,7], metabolic diseases [8], aging and cancer [9]. It is also essential for the diagnosis of primary mitochondrial diseases [10].

Mitochondrial redox function in tissues has been historically studied in preparations of isolated mitochondria [11,12] and for some studies in submitochondrial particles [13]. Studies with isolated mitochondria can provide important data on the activity of the electron transport chain, the complexes that compose it [14,15] and the coupling between electron transport and ATP synthesis [16]. However it is a weak

instrument to interpret the role of mitochondria in the context of the cell or a specific parenchyma [17,18]. Thus, in recent years, new methods have been developed to characterize mitochondrial respiratory function using tissue samples [19,20]. Assessment of mitochondrial function in tissue biopsies can be performed with a few mg of tissue per assay [20] and is extremely relevant for a deeper understanding of metabolic changes at a given physiological moment [21–24].

Using tissue samples presents two main obstacles: In first place the plasma membrane of intact cells prevents the access of mitochondrial substrates such as succinate or ADP to the mitochondria [17,22,25]. Hence, selective plasma membrane permeabilization must be carried out. Once the plasma membrane is permeabilized, cytosolic metabolites and soluble enzymes are lost and the composition of the intracellular space is equilibrated with the incubation medium.

Another relevant limitation is that mitochondrial function assessment requires oxygen consumption measures to be performed immediately after the sample is taken, to ensure that the activity of the electron transport complexes and mitochondrial coupling are preserved. Studies involving a large number of individuals or samples obtained at locations distant from research facilities are often excluded,

**Abbreviations:** ADP, adenosine diphosphate; ATP, adenosine triphosphate; Ant A, antimycin A; Bak, BCL-2 antagonist killer 1; cyt *c*, cytochrome *c*; DMSO, dimethylsulfoxide; EGTA, ethylene glycol-bis(β-aminoethyl ether)-N,N,N',N'-tetraacetic acid; FCCP, carbonyl cyanide-4-(trifluoromethoxy)phenylhydrazone; Glu/Mal, glutamate and malate; HEPES, 4-(2-hydroxyethyl)-1-piperazineethanesulfonic acid; MOPS, 3-(N-morpholino)propanesulfonic acid; Oligo, oligomycin; RCR, respiratory control ratio; Rot, rotenone; Succ, succinate; VDAC, voltage-dependent anion channel

\* Correspondence to: Center for Free Radical and Biomedical Research (CEINBIO) and Departamento de Bioquímica, Facultad de Medicina, Universidad de la República, Avenida General Flores 2125, Montevideo 11800, Uruguay.

E-mail addresses: [celiq@fmed.edu.uy](mailto:celiq@fmed.edu.uy) (C. Quijano), [acassina@fmed.edu.uy](mailto:acassina@fmed.edu.uy) (A. Cassina).

<https://doi.org/10.1016/j.redox.2018.03.008>

Received 21 February 2018; Received in revised form 9 March 2018; Accepted 13 March 2018

Available online 22 March 2018

2213-2317/ © 2018 The Authors. Published by Elsevier B.V. This is an open access article under the CC BY-NC-ND license (<http://creativecommons.org/licenses/by-nc-nd/4.0/>).

since it is not possible to assure that the mitochondria are structurally and functionally intact after a short period of time. The ability to store such samples and recover them at a later time without causing damage to the structure and/or function becomes imperative [26].

So far there are very few compelling published data of tissue cryopreservation for the subsequent study of mitochondrial function. Cold storage of liver biopsies in ice cold medium preserves mitochondrial function of liver biopsies for only 60 min [27]. Cryopreservation of human skeletal muscle in media containing the cryoprotectant dimethyl sulfoxide showed conflicting results regarding its ability to preserve mitochondrial function [28,29]. Only a single study storing purified mitochondria in 10% (v/v) dimethyl sulfoxide (DMSO) at  $-80^{\circ}\text{C}$  and allowing samples to cool at a uniform rate of  $\approx 1^{\circ}\text{C}/\text{min}$ , showed intact structure and function of cryopreserved rat cortical mitochondria [26].

Herein, we present a detailed protocol to cryopreserve and study mitochondrial respiratory function in freeze-thawed permeabilized liver biopsies.

## 2. Methods

### 2.1. Tissue collection

Samples were obtained from six multiparous Holstein cows, in late lactation, with an approximate weight of  $560 \pm 50$  kg and  $2.5 \pm 0.25$  body condition score units; and five Wistar female rats weighing approximately 500–600 g. Liver biopsies were obtained using a 14-gauge biopsy needle (Tru-Core®-II Automatic Biopsy Instrument; Angiotech, Lausanne, Switzerland) as previously described [27,30] and washed in ice-cold modified MIR05 medium (0.5 mM EGTA, 3 mM  $\text{MgCl}_2 \cdot 6\text{H}_2\text{O}$ , 60 mM MOPS, 20 mM taurine, 10 mM  $\text{KH}_2\text{PO}_4$ , 20 mM HEPES, 110 mM sucrose, 1 g/L BSA, pH 7.1) [24] to washout excess blood. Previous findings have proved that biopsy samples obtained by this procedure are equivalent to wedge biopsies and that samples as small as 2 mg can be used [27]. All animal procedures were approved by the Animal Experimentation Committee of Universidad de la República (UdelaR), Montevideo, Uruguay.

### 2.2. Cryopreservation

For cryopreservation, up to 10 mg of liver biopsies were immersed in cryotubes containing 1 mL of ice-cold modified University of Wisconsin solution [31] (20 mM histidine, 20 mM succinate, 3 mM glutathione, 1  $\mu\text{M}$  leupeptin, 2 mM glutamate, 2 mM malate, 2 mM ATP, 0.5 mM EGTA, 3 mM  $\text{MgCl}_2 \cdot 6\text{H}_2\text{O}$ , 60 mM MOPS, 20 mM taurine, 10 mM  $\text{KH}_2\text{PO}_4$ , 20 mM HEPES, 110 mM sucrose, 1 g/L BSA and 10% (v/v) DMSO).

The biopsies were then cryopreserved following a sequential freezing method, where decreasing temperatures were applied, to preserve cellular function. DMSO was added immediately before cryopreservation to each cryovial. Samples were left 6 min in ice, at approximately  $2-4^{\circ}\text{C}$ . Then they were transferred to a canister and placed at the neck tube of a 20 L liquid nitrogen tank (MVE series 2001 – Doble 20) at approximately 10–15 cm from the top, without inserting the cap plug and with a closed lid for 10 min, where they were exposed to nitrogen vapors at  $-110^{\circ}\text{C}$ . Finally, samples were placed in the inner vessel of the tank and submerged in liquid nitrogen at approximately  $-196^{\circ}\text{C}$  for at least 10 min (Fig. 1). These cryopreserved samples could be transported in liquid nitrogen from one location to another.

Alternatively we tried freezing the samples using the same cryopreservation medium but immediately submerging them in liquid nitrogen after collection. In order to differentiate between one method and the other, the latter samples were named frozen samples.

Frozen and cryopreserved samples were kept at  $-80^{\circ}\text{C}$  and analyzed after 2–3 months of storage. Special care was taken to compare these two procedures, for this frozen and cryopreserved biopsies from the same animal were stored for the same time and analyzed the same day.

Samples were thawed placing the tubes under running water. Once the cryopreservation medium was completely thawed samples were immediately transferred to a petri dish and washed thoroughly, with at least 20 mL per biopsy of ice-cold modified MIR05 medium.

### 2.3. Permeabilization

Three permeabilization techniques have been described up to date: mechanical permeabilization, chemical permeabilization and freeze-thaw permeabilization.

Mechanical tissue permeabilization is carried out by dissecting the tissue with sharp forceps and it has been used with prostate and liver tissue [20,32]. In the case of chemical permeabilization, agents such as digitonin and saponin have been used. Titration of the optimal concentration of these compounds is required to assure an increase in the permeability of the plasma membrane but leaving intracellular structures, in particular mitochondria, intact [18,33].

Permeabilization by freeze-thawing has been described in cardiac and skeletal muscle fibers and cells [28,34]. Since cryopreservation implies freezing and thawing the samples for their posterior use, in this case the addition of chemical agents for permeabilization was not necessary.

On the other hand fresh liver biopsies (2–10 mg) were permeabilized in ice-cold MIR05 medium with saponin ( $50 \mu\text{g mL}^{-1}$ ) for 20 min [33]. After permeabilization samples were transferred to a petri dish and washed thoroughly, with at least 20 mL per biopsy of ice-cold modified MIR05 medium, and immediately analyzed.

Plasma membrane permeabilization can be verified observing if mitochondrial oxygen consumption rate responds quickly to changes in concentrations of substrates or other effectors, that in absence of a permeabilizing agent would be incapable of traversing the plasma membrane [17,21,24,25].

### 2.4. Oxygen consumption rate measurements

Oxygen consumption rates were measured in a high-resolution respirometer OROBOROS Oxygraph –2k at  $37^{\circ}\text{C}$ . The electrodes were calibrated in modified MIR05 respiration medium, with a calculated saturated oxygen concentration of  $191 \mu\text{M}$  at 100 kPa barometric pressure [25]. Oxygen consumption rates (respiratory rates or oxygen fluxes) were calculated using the DatLab 4 analysis software ( $\text{pmol O}_2 \text{min}^{-1} \text{mL}^{-1}$ ).

The liver samples were weighted before adding the tissue into the chamber. The average mass of liver tissue used in the assays varied between 2 and 10 mg. The experimental protocol started measuring the oxygen consumption rate of the biopsy in modified MIR05 respiration medium without the addition of substrates or inhibitors. We then measured the steady-state oxygen flux obtained after the sequential addition of specific substrates: 10 mM glutamate and 5 mM malate for complex I evaluation or 20 mM succinate for complex II evaluation and 4 mM adenosine diphosphate (ADP). Oxygen consumption rate was also measured after inhibiting ATP synthase with oligomycin ( $2 \mu\text{M}$ ), and after uncoupling oxidative phosphorylation with carbonyl cyanide p-trifluoromethoxyphenylhydrazone (FCCP). Maximum uncoupling was obtained titrating FCCP concentrations used in the assay up to optimum concentrations in the range of 2–4  $\mu\text{M}$  FCCP. Finally, respiration was inhibited by addition of 0.5  $\mu\text{M}$  rotenone (complex I inhibitor) and 2.5  $\mu\text{M}$  antimycin A (complex III inhibitor). This assay was completed within 45 min approximately.

Fig. 2A and B show representative curves obtained using the protocol for complex I or II specific substrates, respectively. Oxygen consumption rate increased immediately after the addition of substrates confirming that the biopsies were permeabilized. As can be observed in these figures, oxygen consumption rates were practically unchanged by our cryopreservation method. Fresh and cryopreserved samples presented very similar respiratory profiles, while biopsies that were frozen

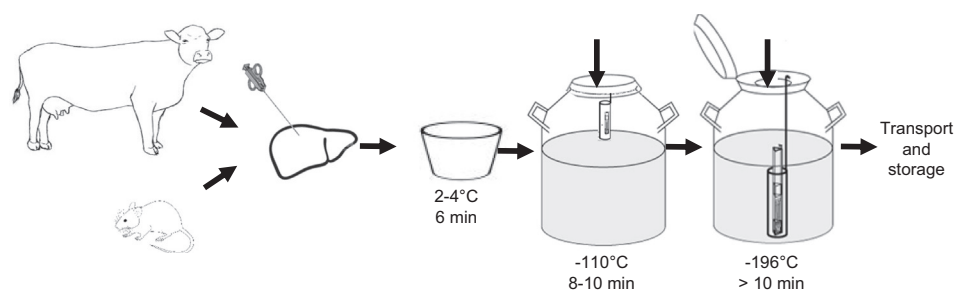


**Fig. 1. Cryopreservation of samples.** The figure shows how liver biopsies in vials containing cryopreservation media were transferred first to a cooler with ice (approximately 2–4 °C), then exposed to nitrogen vapors at the neck tube of a liquid nitrogen tank (–110 °C) and finally were submerged in liquid nitrogen (–196 °C), in order to achieve a gradual and slow freezing of the samples. After this procedure samples were ready for transport and storage at –80 °C.

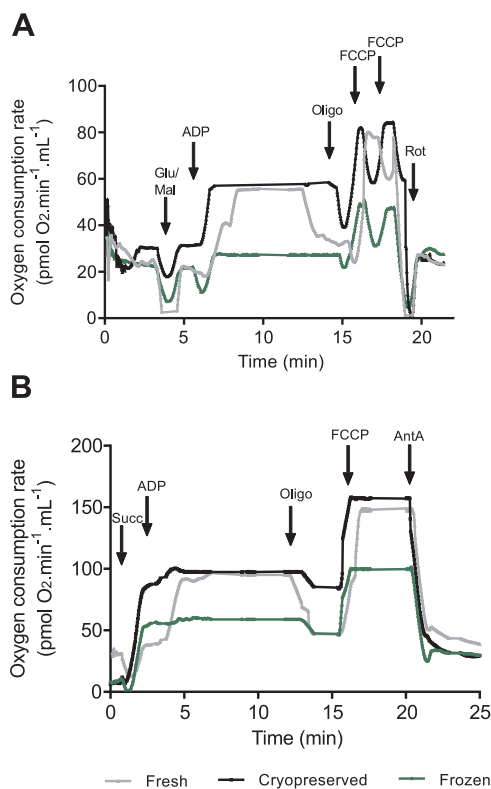


**Fig. 2. Evaluation of mitochondrial function with specific substrates for complex I or II.** Respiration rates were measured at 37 °C. Fresh samples are shown in grey, cryopreserved samples in black and frozen samples in green. (A) Oxygen consumption rates were measured after the sequential addition of 10 mM glutamate and 5 mM malate (Glu/Mal), 4 μM ADP, 2 μM oligomycin (Oligo), up to 4 μM FCCP and 0.5 μM rotenone (Rot). (B) Oxygen consumption rates were measured after addition of 20 mM succinate (Succ), 4 μM ADP, 2 μM oligomycin (Oligo) 4 μM FCCP and 2.5 μM antimycin A (Ant A).

straightaway (not sequentially) presented much lower respiration rates.

### 2.5. Respiratory parameters and indices

Respiratory parameters were obtained from high-resolution respirometry experiments as shown in Fig. 3. Non-mitochondrial oxygen consumption (e), obtained after inhibition of the electron transport chain, was subtracted from all values; and respiratory parameters and indices were calculated as described by previous authors [5,18,25,35]. Oxygen consumption rates (rates) were expressed in  $\text{pmol O}_2 \text{ min}^{-1} \text{ mL}^{-1}$ ; the volume of the chamber (V) was 2.4 mL in all cases, and the weight of the biopsy (sample weight) was expressed in mg:

(a) State 4 respiration in presence of complex I or II specific substrates:

$$\text{State 4 respiration} = \frac{\text{rate}(a). V}{\text{sample weight}}$$

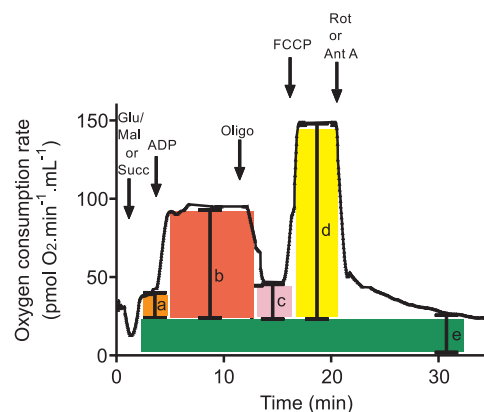


**Fig. 3. Acquisition of respiratory parameters from a high-resolution respirometry experiment.** A schematic representation of a graph obtained as described in Fig. 1 is shown. Non-mitochondrial oxygen consumption (e) was subtracted from all values: (a) state 4 respiration; (b) state 3; (c) oligomycin-resistant respiration; (d) maximum respiratory rate.

(b) State 3 respiration after the addition of ADP that resembles the basal respiration<sup>1</sup> of the tissue at saturating concentrations of substrates and ADP:

$$\text{State 3 respiration} = \frac{\text{rate}(b). V}{\text{sample weight}}$$

(c) Oligomycin-resistant respiration, also known as ATP-independent respiration, due to proton leak or transport of charged molecules across the inner mitochondrial membrane:

$$\text{Oligomycin - resistant respiration} = \frac{\text{rate}(c). V}{\text{sample weight}}$$

(d) Maximum respiratory rate, obtained after dissipation of the proton gradient by an uncoupler, depends on the activity of the electron transport complexes and the quantity of mitochondria in the tissue:

$$\text{Maximum respiratory rate} = \frac{\text{rate}(d). V}{\text{sample weight}}$$

(e) Non-mitochondrial oxygen consumption rate, may be associated to oxidation reactions mediated by reactive oxygen species or oxidases [5,36,37]:

$$\text{Non - mitochondrial oxygen consumption rate} = \frac{\text{rate}(e). V}{\text{sample weight}}$$

Oligomycin-sensitive respiration was calculated as the difference

<sup>1</sup> Basal respiration is strongly dependent on ADP levels, that are mostly controlled by energy demands [5].

**Table 1**  
Complex I-dependent respiratory parameters.

Species	Storage conditions	State 4 respiration <sup>a</sup>	State 3 respiration <sup>a</sup>	Oligomycin resistant respiration <sup>a</sup>	Oligomycin sensitive respiration <sup>a</sup>	Maximum respiratory rate <sup>a</sup>	Non-mitochondrial oxygen consumption rate <sup>a</sup>	Spare respiratory capacity <sup>a</sup>	Respiratory control ratio	Coupling efficiency
Cow	Fresh	3 ± 1	15 ± 2	5 ± 2	13 ± 1	18 ± 2	6 ± 2	3 ± 1	6 ± 1	0.44 ± 0.06
	Cryopreserved	2.6 ± 0.2	16 ± 1	7 ± 2	9 ± 1	16 ± 2	6.7 ± 2	3 ± 1	5.5 ± 0.2	0.54 ± 0.05
	Frozen	5 ± 2*	4 ± 2 <sup>†</sup>	29 ± 7**	4 ± 1*	10 ± 1 <sup>†</sup>	12 ± 5*	6 ± 1*	1.8 ± 0.2**	0.25 ± 0.1 <sup>†</sup>
Rat	Fresh	5 ± 2	8 ± 1	–	–	–	5 ± 1	–	6 ± 1	–
	Cryopreserved	5 ± 2	9 ± 1	–	–	–	6 ± 2	–	4.2 ± 0.4	–

The different respiratory parameters were obtained from oxygen consumption rate measurements performed as described in Fig. 2A. All results are expressed as mean ± standard error. Unpaired *t*-tests were performed using GraphPad Prism v. 6.0 (GraphPad, La Jolla, CA). Significance was set at *P* < 0.05 for all analyses.

\* *P* < 0.05.

\*\* *P* < 0.01 indicate significant differences between fresh samples and treatments (*n* = 4–6).

<sup>a</sup> Respiratory parameters are expressed as pmol O<sub>2</sub> min<sup>-1</sup> mg<sup>-1</sup>.

**Table 2**  
Complex II-dependent respiratory parameters.

Species	Storage conditions	State 4 respiration <sup>a</sup>	State 3 respiration <sup>a</sup>	Oligomycin resistant respiration <sup>a</sup>	Oligomycin sensitive respiration <sup>a</sup>	Maximum respiratory rate <sup>a</sup>	Non-mitochondrial oxygen consumption rate <sup>a</sup>	Spare respiratory capacity <sup>a</sup>	Respiratory control ratio	Coupling efficiency
Cow	Fresh	22 ± 9	55 ± 7	22 ± 5	8 ± 2	86 ± 9	5 ± 2	40 ± 7	3.6 ± 0.6	0.5 ± 0.05
	Cryopreserved	24 ± 9	58 ± 4	41 ± 17*	9 ± 1	75 ± 9	6 ± 2	33 ± 4	2.2 ± 0.2**	0.23 ± 0.02***
	Frozen	17 ± 2	22 ± 4 <sup>†</sup>	34 ± 10*	5 ± 1	41 ± 4 <sup>†</sup>	8 ± 2 <sup>†</sup>	24 ± 5	1.5 ± 0.1****	0.2 ± 0.04****
Rat	Fresh	14 ± 2	50 ± 9	–	–	–	6 ± 2	–	3 ± 0.5	–
	Cryopreserved	17 ± 5 <sup>†</sup>	40 ± 5	–	–	–	8 ± 2	–	2 ± 0.2 <sup>†</sup>	–

The different respiratory parameters were obtained from oxygen consumption rate measurements performed as described in Fig. 2B. All results are expressed as mean ± standard error. Unpaired *t*-tests were performed using GraphPad Prism v. 6.0 (GraphPad, La Jolla, CA). Significance was set at *P* < 0.05 for all analyses.

\* *P* < 0.05.

\*\* *P* < 0.01.

\*\*\* *P* < 0.001.

\*\*\*\* *P* < 0.0001 indicate significant differences between fresh samples and treatments (*n* = 4–6).

<sup>a</sup> Respiratory parameters are expressed as pmol O<sub>2</sub> min<sup>-1</sup> mg<sup>-1</sup>.

between state 3 respiration and oligomycin-resistant respiration obtained after inhibition of ATP synthase, and represents oxygen consumption linked to ADP phosphorylation [5,16]:

$$\text{Oligomycin - sensitive respiration} = \frac{(\text{rate}(b) - \text{rate}(c)) \cdot V}{\text{sample weight}}$$

Spare respiratory capacity was calculated as the difference between the maximum respiratory rate and state 3 respiration. This parameter represents the ability of the electron transport chain to respond to an increase in energy demands and/or to resist an insult, and informs on the bioenergetic flexibility of the tissue [5]:

$$\text{Spare respiratory capacity} = \frac{(\text{rate}(d) - \text{rate}(b)) \cdot V}{\text{sample weight}}$$

The respiratory control ratio (RCR) was calculated as the ratio between state 3 and state 4 respiration rates [38]:

$$\text{Respiratory control ratio} = \frac{\text{rate}(b)}{\text{rate}(a)}$$

A high ratio represents strong coupling between ATP synthesis and electron transport. Similar information can be obtained calculating the coupling efficiency ratio [5]:

$$\text{Coupling efficiency ratio} = \frac{\text{rate}(b) - \text{rate}(c)}{\text{rate}(b)}$$

Comparison of the respiratory parameters and indices obtained in cryopreserved and fresh hepatic biopsies is shown in Tables 1 and 2.

Most respiratory parameters remained unchanged with respect to fresh samples, for both complex I and II substrates: State 4 and state 3 respiration, maximum respiratory rate, spare respiratory capacity and non-mitochondrial oxygen consumption were not significantly different. Moreover some parameters appeared to be slightly higher in cryopreserved than in fresh samples (state 3 and 4, Tables), although no statistical differences could be found. The latter could be due to differences in the permeabilization techniques.

Oligomycin-resistant and oligomycin-sensitive respiration were not affected by cryopreservation, when assessing mitochondrial function with complex I substrates, allowing us to calculate the respiratory control ratio along with coupling efficiency. However we noted significant differences in these parameters, between fresh and cryopreserved samples, when the experiments were performed using the complex II substrate, succinate. We thus conclude that the protocol with complex I specific substrates is more robust than the one with succinate, though the reasons behind these differences are not clear to us.

As can be appreciated from Tables 1 and 2, while our cryopreservation technique was very efficient maintaining mitochondrial function, immediate freezing of the samples was not, since almost all respiratory parameters were impaired by this procedure. As mentioned before frozen samples were immersed in the same media as cryopreserved samples, and the main difference between the protocols was the sequential versus immediate freezing of the biopsies, underscoring the relevance of this step for the success of the protocol.

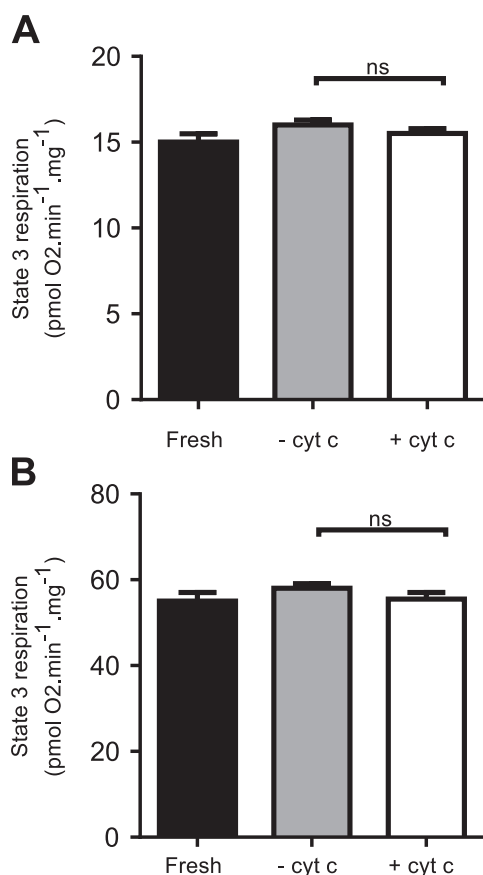


**Fig. 4. Assessment of mitochondrial outer membrane integrity by addition of cytochrome *c*.** State 3 respiration dependent on complex I (A) and II (B) substrates obtained as described in Fig. 2A and B respectively. The black bars represent state 3 respiration for fresh samples, grey bars show state 3 respiration for cryopreserved samples without the addition of cytochrome *c* and white bars represent state 3 respiration with the addition of 10  $\mu$ M cytochrome *c*. Unpaired *t*-tests were performed using GraphPad Prism v. 6.0 (GraphPad, La Jolla, CA). Significance was set at  $P < 0.05$  for all analyses, ns stands for not significant ( $n = 12$ ).

## 2.6. Controlling outer mitochondrial membrane integrity

Since the outer mitochondrial membrane can be easily damaged by cryopreservation, we tested its integrity in cryopreserved samples with the addition of cytochrome *c*. Unlike other cytochromes, cytochrome *c* is loosely bound to the mitochondrial inner membrane and damage of the outer membrane can lead to the release of this protein to the cytosol and to its loss during permeabilization. The latter can be evidenced by an increase in oxygen consumption linked to cytochrome *c* addition. Although some authors have argued that cytochrome *c* release can be mediated by Bak and VDAC forming pores rather than by non-specific rupture [39], this is a widely used technique to determine the intactness of the outer mitochondrial membrane [18,26,28,29].

Therefore state 3 respiration of cryopreserved samples was assessed with and without cytochrome *c* addition (10  $\mu$ M) (Fig. 4). No significant differences were found, suggesting that the outer membrane was unharmed by the procedure. The ratio between state 3 respiration with and without cytochrome *c* was 0.96 for both complex I and II protocols, similar to that reported by others [26,28,29].

## 3. Concluding remarks

In sum, herein we present an effective method to cryopreserve small liver biopsies for in situ assessment of mitochondrial function. Our

protocol will enable the transport and storage of samples, facilitating the analysis of biopsies obtained at locations away from research centers. It will also allow performing experiments with a large number of individuals, analysis of the same samples by different laboratories, banking and comparison of tissues obtained at different times and locations,

## Acknowledgements

This study was supported by the Agencia Nacional de Investigación e Innovación (ANII) (FSA\_1\_2013\_1\_12612).

M. García-Roche and A. Casal were supported by ANII fellowships (POS\_NAC\_2015\_1\_110049 and POS\_NAC\_2014\_1\_102302, respectively). A. Cassina, C. Quijano and R. Radi were partially funded by grants of the Espacio Interdisciplinario – Centros, UDELAR 2015. A. Cassina and R. Radi were also supported by the grant CSIC grupos I + D 2014 (767).

## Conflict of interest

The authors declare that they have no conflicts of interest with the contents of this article.

## Author contributions

M. García-Roche, C. Quijano and A. Cassina conceived, designed and analyzed most of the experiments and wrote the manuscript. M. García-Roche performed all of the experiments. A. Casal participated in the collection and cryopreservation of the samples. R. Radi critically analyzed the results and corrected versions of the manuscript and M. Carriquiry critically analyzed the results. All authors reviewed the results and approved the final version of the manuscript.

## References

- [1] C. Quijano, M. Trujillo, L. Castro, A. Trostchansky, Interplay between oxidant species and energy metabolism, *Redox Biol.* 8 (2016) 28–42, <http://dx.doi.org/10.1016/j.redox.2015.11.010>.
- [2] R. Radi, A. Cassina, R. Hodara, C. Quijano, L. Castro, Peroxynitrite reactions and formation in mitochondria, *Free Radic. Biol. Med.* 33 (2002) 1451–1464, [http://dx.doi.org/10.1016/S0891-5849\(02\)01111-5](http://dx.doi.org/10.1016/S0891-5849(02)01111-5).
- [3] S.L. Budd, D.G. Nicholls, Mitochondria, calcium regulation, and acute glutamate excitotoxicity in cultured cerebellar granule cells, *J. Neurochem.* 67 (1996) 2282–2291.
- [4] D.R. Green, J.C. Reed, Mitochondria and apoptosis, *Science* 281 (1998) 1309–1312, <http://dx.doi.org/10.1126/science.281.5381.1309>.
- [5] M.D. Brand, D.G. Nicholls, Assessing mitochondrial dysfunction in cells, *Biochem. J.* 435 (2011) 297–312, <http://dx.doi.org/10.1042/BJ4370575u> (575.1–575).
- [6] E. Miquel, A. Cassina, L. Martínez-Palma, J.M. Souza, C. Bolatto, S. Rodríguez-Bottero, A. Logan, R. a.J. Smith, M.P. Murphy, L. Barbeito, R. Radi, P. Cassina, Neuroprotective effects of the -targeted MitoQ in a mitochondrial model of inherited amyotrophic lateral sclerosis, *Free Radic. Biol. Med.* 70 (2014) 204–213, <http://dx.doi.org/10.1016/j.freeradbiomed.2014.02.019>.
- [7] P. Cassina, A. Cassina, M. Pehar, R. Castellanos, M. Gandelman, D. Leo, K.M. Robinson, R.P. Mason, J.S. Beckman, L. Barbeito, R. Radi, Mitochondrial dysfunction in SOD1 G93A-bearing astrocytes promotes motor neuron degeneration: prevention by mitochondrial-targeted antioxidants, *Neurobiol. Dis.* 28 (2008) 4115–4122, <http://dx.doi.org/10.1523/JNEUROSCI.5308-07.2008>.
- [8] F. Nassir, J. Ibdah, Role of mitochondria in nonalcoholic fatty liver disease, *Int. J. Mol. Sci.* 15 (2014) 8713–8742, <http://dx.doi.org/10.3390/ijms15058713>.
- [9] A.V. Kudryavtseva, G.S. Krasnov, A.A. Dmitriev, B.Y. Alekseev, O.L. Kardymon, A.F. Sadritdinova, M.S. Fedorova, A.V. Pokrovsky, N.V. Melnikova, A.D. Kaprin, A.A. Moskalev, A.V. Snezhkina, Mitochondrial dysfunction and oxidative stress in aging and cancer, *Oncotarget* 7 (2016) 44879–44905, <http://dx.doi.org/10.18632/oncotarget.9821>.
- [10] S. Parikh, A. Goldstein, M.K. Koenig, F. Scaglia, G.M. Enns, R. Saneto, I. Anselm, B.H. Cohen, M.J. Falk, C. Greene, A.L. Gropman, R. Haas, Diagnosis and management of mitochondrial disease: a consensus statement from the mitochondrial medicine society, *Genet. Med.* 17 (2016) 689–701, <http://dx.doi.org/10.1038/gim.2014.177>.
- [11] A. Boveris, E. Cadenas, A.O. Stoppani, Role of ubiquinone in the mitochondrial generation of hydrogen peroxide, *Biochem. J.* 156 (1976) 435–444, <http://dx.doi.org/10.1042/bj1560435>.
- [12] T.A. Young, C.C. Cunningham, S.M. Bailey, Reactive oxygen species production by the mitochondrial respiratory chain in isolated rat hepatocytes and liver

- mitochondria: studies using myxothiazol, *Arch. Biochem. Biophys.* 405 (2002) 65–72, <http://dx.doi.org/10.1016/j.abb.2010.06.012>.
- [13] J.F. Turrens, A. Boveris, Generation of superoxide anion by the NADH dehydrogenase of bovine heart mitochondria, *Biochem. J.* 191 (1980) 421–427, <http://dx.doi.org/10.1042/bj1910421>.
- [14] A. Cassina, R. Radi, Differential inhibitory action of nitric oxide and peroxynitrite on mitochondrial electron transport, *Arch. Biochem. Biophys.* 328 (1996) 309–316, <http://dx.doi.org/10.1006/abbi.1996.0178>.
- [15] A.J.Y. Jones, J. Hirst, A spectrophotometric coupled enzyme assay to measure the activity of succinate dehydrogenase, *Anal. Biochem.* 442 (2013) 19–23, <http://dx.doi.org/10.1016/j.ab.2013.07.018>.
- [16] I.R. Lanza, K.S. Nair, Functional assessment of isolated mitochondria in vitro, *Methods Enzymol.* 457 (2009) 349–372, [http://dx.doi.org/10.1016/S0076-6879\(09\)05020-4](http://dx.doi.org/10.1016/S0076-6879(09)05020-4).
- [17] A.V. Kuznetsov, V. Veksler, F.N. Gellerich, V. Saks, R. Margreiter, W.S. Kunz, Analysis of mitochondrial function in situ in permeabilized muscle fibers, tissues and cells, *Nat. Protoc.* 3 (2008) 965–976, <http://dx.doi.org/10.1038/nprot.2008.61>.
- [18] J.K. Salabei, A.A. Gibb, B.G. Hill, Comprehensive measurement of respiratory activity in permeabilized cells using extracellular flux analysis, *Nat. Protoc.* 9 (2014) 421–438, <http://dx.doi.org/10.1007/s11103-011-9767-z>.
- [19] M. Spinazzi, A. Casarin, V. Pertegato, L. Salviati, C. Angelini, Assessment of mitochondrial respiratory chain enzymatic activities on tissues and cultured cells, *Nat. Protoc.* 7 (2012) 1235–1246, <http://dx.doi.org/10.1038/nprot.2012.058>.
- [20] A.V. Kuznetsov, D. Strobl, E. Ruttman, A. Königsrainer, R. Margreiter, E. Gnaiger, Evaluation of Mitochondrial Respiratory Function in Small Biopsies of Liver, *Anal. Biochem.* 305 (2002) 186–194, <http://dx.doi.org/10.1006/abio.2002.5658>.
- [21] H. Unterluggauer, A. Garedeu, E. Hu, High-resolution respirometry – a modern tool in aging research, *Exp. Gerontol.* 41 (2006) 103–109, <http://dx.doi.org/10.1016/j.exger.2005.09.011>.
- [22] C.D. Velasco, A. Draxl, A. Wiethüchter, A. Eigentler, E. Gnaiger, O2k-protocols mitochondrial respiration in permeabilized fibres versus homogenate from trout heart and liver, *Mitochondrial Physiol. Netw.* 12 (2013) 1–11.
- [23] E.J. Vazquez, J.M. Berthiaume, V. Kamath, O. Achike, E. Buchanan, M.M. Montano, M.P. Chandler, M. Miyagi, M.G. Rosca, Mitochondrial complex I defect and increased fatty acid oxidation enhance protein lysine acetylation in the diabetic heart, *Cardiovasc. Res.* 107 (2015) 453–465, <http://dx.doi.org/10.1093/cvr/cvv183>.
- [24] E. Gnaiger, Polarographic oxygen sensors, the oxygraph, and high-resolution respirometry to assess mitochondrial function, in: J.A. Dykens, I. Will (Eds.), *Mitochondrial Dysfunction in Drug Induced Toxicity*, Wiley & Sons, Inc, New Jersey, 2008, pp. 326–353.
- [25] D. Pesta, E. Gnaiger, High-resolution respirometry: OXPHOS protocols for human cells and permeabilized fibers from small biopsies of human muscle, *Methods Mol. Biol.* 810 (2012) 25–58, [http://dx.doi.org/10.1007/978-1-61779-382-0\\_3](http://dx.doi.org/10.1007/978-1-61779-382-0_3).
- [26] V.N. Nukala, I.N. Singh, L.M. Davis, P.G. Sullivan, Cryopreservation of brain mitochondria: a novel methodology for functional studies, *J. Neurosci. Methods* 152 (2006) 48–54, <http://dx.doi.org/10.1016/j.jneumeth.2005.08.017>.
- [27] M.J.J. Chu, A.R.J. Phillips, A.W.G. Hosking, J.R. Macdonald, A.S.J.R. Bartlett, A.J.R. Hickey, Hepatic mitochondrial function analysis using needle liver biopsy samples, *PLoS ONE* 8 (2013) e79097, <http://dx.doi.org/10.1371/journal.pone.0079097>.
- [28] A.V. Kuznetsov, W.S. Kunz, V. Saks, Y. Usson, J. Mazat, T. Letellier, F.N. Gellerich, R. Margreiter, Cryopreservation of mitochondria and mitochondrial function in cardiac and skeletal muscle fibers, *Anal. Biochem.* 319 (2003) 296–303, [http://dx.doi.org/10.1016/S0003-2697\(03\)00326-9](http://dx.doi.org/10.1016/S0003-2697(03)00326-9).
- [29] S. Larsen, C. Wright-paradis, E. Gnaiger, J.W. Helge, Cryopreservation of human skeletal muscle impairs mitochondrial function, *Cryoletters* 33 (2012) 169–175.
- [30] M. Carriquiry, W.J. Weber, S.C. Fahrenkrug, B.A. Crooker, Hepatic gene expression in multiparous Holstein cows treated with bovine somatotropin and fed n-3 fatty acids in early lactation, *J. Dairy Sci.* 92 (2009) 4889–4900, <http://dx.doi.org/10.3168/jds.2008-1676>.
- [31] K. Sakata, Y. Kawashima, H. Ichikawa, T. Oya, T. Takahashi, A. Otaki, S. Ishikawa, Y. Morishita, University of Wisconsin solution versus modified Collins solution for canine heart preservation: an experimental study, *Int. J. Angiol.* 6 (1997) 176–179, <http://dx.doi.org/10.1007/s005479900032>.
- [32] B. Schöpf, G. Schäfer, A. Weber, H. Talasz, I.E. Eder, H. Klocker, E. Gnaiger, Oxidative phosphorylation and mitochondrial function differ between human prostate tissue and cultured cells, *FEBS J.* 283 (2016) 2181–2196, <http://dx.doi.org/10.1111/febs.13733>.
- [33] A.V. Kuznetsov, V. Veksler, F.N. Gellerich, V. Saks, R. Margreiter, W.S. Kunz, Analysis of mitochondrial function in situ in permeabilized muscle fibers, tissues and cells, *Nat. Protoc.* 3 (2008) 965–976, <http://dx.doi.org/10.1038/nprot.2008.61>.
- [34] G. Mardones, A. González, Selective plasma membrane permeabilization by freeze-thawing and immunofluorescence epitope access to determine the topology of intracellular membrane proteins, *J. Immunol. Methods* 275 (2003) 169–177, [http://dx.doi.org/10.1016/S0022-1759\(03\)00015-2](http://dx.doi.org/10.1016/S0022-1759(03)00015-2).
- [35] B.G. Hill, G.A. Benavides, J.R.L. Jr, S. Ballinger, L.D. Italia, J. Zhang, V.M. Darley-usmar, Integration of cellular bioenergetics with mitochondrial quality control and autophagy, *Biol. Chem.* 393 (2012) 1485–1512, <http://dx.doi.org/10.1515/hsz-2012-0198>.
- [36] B.K. Chacko, P.A. Kramer, S. Ravi, G.A. Benavides, T. Mitchell, B.P. Dranka, D. Ferrick, A.K. Singal, S.W. Ballinger, S.M. Bailey, R.W. Hardy, J. Zhang, D. Zhi, V.M. Darley-USmar, The bioenergetic health index: a new concept in mitochondrial translational research, *Clin. Sci.* 127 (2014) 367–373, <http://dx.doi.org/10.1042/CS20140101>.
- [37] P.A. Kramer, B.K. Chacko, S. Ravi, M.S. Johnson, T. Mitchell, V.M. Darley-USmar, Bioenergetics and the oxidative burst: protocols for the isolation and evaluation of human leukocytes and platelets, *J. Vis. Exp.* 85 (2014), <http://dx.doi.org/10.3791/51301>.
- [38] B. Chance, G. Williams, W. Holmes, J. Higgins, Respiratory enzymes in oxidative phosphorylation, *J. Biol. Chem.* 217 (1955) 409–428 <<http://www.jbc.org/>>.
- [39] R. Clayton, J.B. Clark, M. Sharpe, Cytochrome c release from rat brain mitochondria is proportional to the mitochondrial functional deficit: implications for apoptosis and neurodegenerative disease, *J. Neurochem.* 92 (2005) 840–849, <http://dx.doi.org/10.1111/j.1471-4159.2004.02918.x>.